Charge density functional plus U theory of $LaMnO_3$: Phase diagram, electronic structure, and magnetic interaction

Seung Woo Jang, Siheon Ryee, Hongkee Yoon, and Myung Joon Han
Department of Physics, Korea Advanced Institute of Science and Technology (KAIST), Daejeon 34141, Korea

(Received 14 February 2018; revised manuscript received 17 May 2018; published 13 September 2018)

We perform a charge density functional theory plus U calculation of $LaMnO_3$. While all the previous calculations were based on spin density functionals, our results and analysis show that the use of spin-unpolarized charge-only density is crucial to correctly describe the phase diagram, electronic structure, and magnetic property. Using magnetic force linear response calculation, a long-standing issue is further addressed regarding the second-neighbor out-of-plane interaction strength. We also estimate the orbital-resolved magnetic couplings. Remarkably, the interorbital e_g-t_{2g} interaction is quite significant due to the Jahn-Teller distortion and orbital ordering.

DOI: 10.1103/PhysRevB.98.125126

I. INTRODUCTION

$LaMnO_3$, the mother compound of colossal magnetoresistance (CMR) phenomena, is a prototypical material in which charge, spin, orbital, and lattice degrees of freedom are strongly coupled, thereby producing a rich phase diagram [1–6]. Bulk $LaMnO_3$ is an A-type antiferromagnetic (A-AFM) insulator with d_{x^2}/d_{y^2}-like orbital order. Its orthorhombic crystal structure has both $GdFeO_3$-type and cooperative Jahn-Teller distortions. After the celebrated observation of CMR [7,8], $LaMnO_3$ has been a focus of tremendous research activities from various viewpoints [9–23]. Recently thin-film and heterostructure forms of $LaMnO_3$ have generated new excitement and possibilities [24–34], while their intriguing behaviors driven by introducing charge carriers and/or controlling the dimensionality still need careful investigations [2–6,35,36].

Many first-principles studies have been devoted to this fascinating material for the past two decades [37–46,46–60]. While it is certainly true that first-principles calculations contributed a lot to understanding $LaMnO_3$ and related phenomena, the fully *ab initio* description is still far from being satisfactory. Calculating the correct magnetic ground state and electronic structures has proven to be nontrivial [38,42,45,47,54,59,61]. For example, the microscopic origin of the A-AFM ground state and the electronic nature of its gap have been under debate. The difficulty arises largely from technical challenges such as the determination of interaction parameters and double-counting terms when a density functional theory (DFT) plus U method is used, which has been a main workhorse in the theoretical study. Recently, a series of investigations provided a clear understanding of the difference between DFT + U formalisms [62–65]. In this context, it is important to reestablish the *ab initio* approach for this classical material and its consequences.

In the present work, we reexamine $LaMnO_3$ within a DFT + U framework. In particular, we note that all of the previous calculations have been based on the spin density functional theory (SDFT), while recent investigations have reported that its unphysical nature is largely due to the competition between spin density exchange-correlation energy and a double-counting term [62–65]. From a comparative study, we show that CDFT [(spin-unpolarized charge density functional theory) + U] can resolve the unphysical behavior found in SDFT + U. The CDFT + U calculation with the interaction parameters obtained from the constrained random phase approximation (cRPA) can successfully describe the electronic structure and magnetic property. We also estimate the magnetic exchange coupling constant J_{ij} based on the CDFT + U electronic structure and the response theory. It is shown that the A-AFM spin ground state is well stabilized only by nearest-neighbor interactions, which is in contrast with part of the previous studies. Furthermore, our orbital-resolved J_{ij} calculations show that the e_g-t_{2g} excitation channel gives rise to a significant AFM interaction that has never been clearly noticed before.

II. COMPUTATION DETAILS

We performed density functional theory plus Hubbard U (DFT + U) [66,67] calculations within the generalized gradient approximation (GGA) [68]. Throughout the manuscript, "SDFT" and "CDFT" refer to the spin and charge (spin-unpolarized) density functional scheme, respectively [65]. Thus SDFT + U and CDFT + U refer to the spin-polarized GGA +U and spin-unpolarized GGA + U, respectively. For more details regarding these formulations and their comparisons, see Ref. [65]. The so-called "fully localized limit (FLL)" functional form is adopted [67,69], and $U_{\mathrm{La}\,4f} = 8.0$ eV and $J_{H,\mathrm{La}\,4f} = 0.5$ eV are used for La $4f$ states. If not mentioned otherwise, the crystal structure is fixed to the experimental structure [70]. All of the electronic structure and total energy calculations were carried out with the OPENMX software package [71], which is based on localized pseudoatomic orbitals (LCPAO). Vanderbilt-type norm-conserving pseudopotentials [72] with partial-core corrections [73] were used to replace the deep core potentials. Three s, two p, two

d, and one f orbital were taken as a basis set for La. Three s, two p, and one d orbital were used for Mn. Two s, two p, and one d orbital were used for O. A $9 \times 9 \times 9$ Monkhorst-Pack k-point mesh were used.

In Sec. III, the level splitting Δ is defined to represent the energy difference between the occupied and unoccupied orbitals. For a given orbital α and spin σ, the energy level of occupied states $E^{\rm occ}_{\alpha\sigma}$ is calculated by taking the center-of-mass position of projected density of states (PDOS):

$$E^{\rm occ}_{\alpha\sigma} = \frac{\int_{E_f-x}^{E_f} E g_{\alpha\sigma}(E) dE}{\int_{E_f-x}^{E_f} g_{\alpha\sigma}(E) dE}, \quad (1)$$

where E_f and $g_{\alpha\sigma}(E)$ refer to the Fermi level and the calculated DOS, respectively. The minimum integration range of $E_f - x$ is chosen to include the antibonding Mn $3d$ states only (excluding the bonding combinations) in order to make the quantitative comparison with literature values become straightforward [19,74–76]. The presented results are from $x = 1.8$ and 4.0 eV for e_g and t_{2g} states, respectively. Similarly, the unoccupied level is calculated by

$$E^{\rm unocc}_{\alpha\sigma} = \frac{\int_{E_f}^{\infty} E g_{\alpha\sigma}(E) dE}{\int_{E_f}^{\infty} g_{\alpha\sigma}(E) dE}, \quad (2)$$

and Δ is then given by $E^{\rm unocc}_{\alpha\sigma_1} - E^{\rm occ}_{\beta\sigma_2}$.

The cRPA [77,78] calculation was performed to estimate the interaction parameters by using the ECALJ software package [79]. For the cRPA, we used the cubic structure with a lattice constant of $a = 3.934$ Å, which yields the same volume with the experimental orthorhombic structure. The unphysical screening channels caused by low-lying La $5d$ and La $4f$ bands were removed. The d-d screening near the Fermi energy is excluded based on the so-called "d-dp model" of the maximally localized Wannier function (MLWF) technique [80–82].

The magnetic exchange coupling constant, J_{ij}, has been calculated based on magnetic force linear-response theory (MFT) [83] as extended to our nonorthogonal LCPAO method [84,85]. Throughout the manuscript, we used the following convention for the spin Hamiltonian:

$$H = -\sum_{i \neq j} J_{ij} \mathbf{e}_i \cdot \mathbf{e}_j, \quad (3)$$

where $\mathbf{e}_{i,j}$ refers to the unit spin vectors of atomic sites i and j.

III. RESULT AND DISCUSSION

A. Magnetic phase diagram

Figures 1(a) and 1(b) show the calculated magnetic phase diagram from SDFT + U and CDFT+U, respectively. A remarkable difference is clearly noticed. In SDFT + U, G-AFM is stabilized in the small U and large J_H regime while FM is in large U and small J_H. In CDFT + U, on the other hand, G-AFM is the ground state for the small U and small J_H values. In both phase diagrams, A-AFM order, the experimentally known ground state, is located in between G-AFM and FM. Our cRPA estimation gives $U = 4.0$ eV and

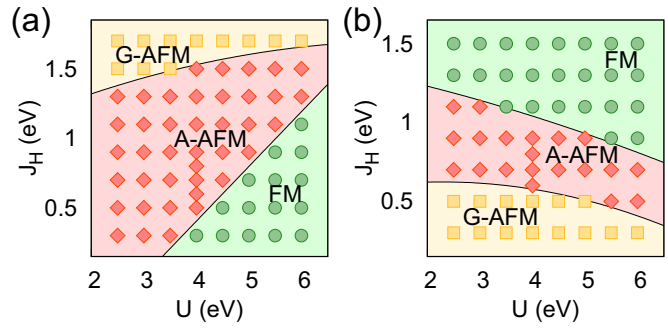

FIG. 1. The calculated magnetic phase diagram by (a) SDFT + U and (b) CDFT + U. Yellow squares, red diamonds, and green circles show the data points corresponding to G-AFM, A-AFM, and ferromagnetic (FM) ground-state spin orders, respectively.

$J_H = 0.7$ eV, which yields the correct A-AFM ground state for both SDFT + U and CDFT + U.

Here we note that the two widely used standard formulations produce a quite different phase diagram for this classical material. In this regard, our result raises a serious question about the predictive power of current methodology. And below, we argue that the CDFT + U solution is physically more reliable being supported by a series of recent studies [62–65]. Notably, all of the previous DFT + U calculations for bulk $LaMnO_3$ have adapted SDFT + U, to the best of our knowledge.

To understand the difference between the two formulations, we performed a systematic analysis whose results are summarized in Fig. 2. First we define the orbital- and spin-dependent energy level splitting Δ [see Fig. 2(a)]. For simplic-

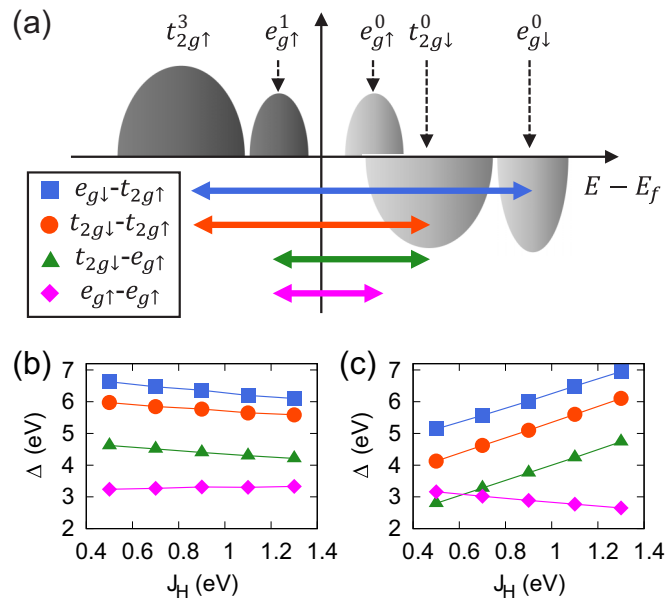

FIG. 2. (a) A schematic DOS near the Fermi energy. The upper and lower panels represent the up- and down-spin states, respectively. The four major excitations of $e_{g\downarrow}$-$t_{2g\uparrow}$, $t_{2g\downarrow}$-$t_{2g\uparrow}$, $t_{2g\downarrow}$-$e_{g\uparrow}$, and $e_{g\uparrow}$-$e_{g\uparrow}$ are depicted by arrows. (b), (c) The calculated Δ as a function of Hund J_H by (b) SDFT + U and (c) CDFT + U.

ity, we denote $\Delta_{e_{g\uparrow}-e_{g\uparrow}}$ by $\Delta_{\uparrow\uparrow}$, and $\Delta_{t_{2g\downarrow}-t_{2g\uparrow}}$, $\Delta_{e_{g\downarrow}-t_{2g\uparrow}}$, and $\Delta_{t_{2g\downarrow}-e_{g\uparrow}}$ by $\Delta_{\downarrow\uparrow}$, Since the magnetic exchange interactions are approximately given by these energy differences through $J \sim t^2/\Delta$ (t denotes the hopping parameter), one can try to understand the phase diagrams in terms of these parameters. As is clearly shown in Figs. 2(b) and 2(c), the calculated Δ exhibits an opposite behavior as a function J_H as formally discussed in Ref. [65]. Namely, $\Delta_{\uparrow\uparrow}$ increases in SDFT + U and decreases in CDFT + U. $\Delta_{\downarrow\uparrow}$ decreases in SDFT + U and increases in CDFT + U.

This observation provides useful information to assess two different functional formulations. It is known that $\Delta_{e_{g\uparrow}-e_{g\uparrow}} \simeq U - 3J_H + \Delta_{\rm JT}$ and $\Delta_{t_{2g\downarrow}-t_{2g\uparrow}} \simeq U + 5J_H/2$, where $\Delta_{\rm JT}$ is the Jahn-Teller splitting [19,75,76]. These expressions indicate that $\Delta_{e_{g\uparrow}-e_{g\uparrow}}$ and $\Delta_{t_{2g\downarrow}-t_{2g\uparrow}}$ should be reduced and enlarged, respectively, as J_H increases. Importantly, these features are only observed in the CDFT + U result of Fig. 2(c). Similarly, $\Delta_{e_{g\downarrow}-t_{2g\uparrow}}$ and $\Delta_{t_{2g\downarrow}-e_{g\uparrow}}$ can be expressed by $U + 3J_H + \Delta_{\rm CF}$ [86] and $U + 3J_H - \Delta_{\rm CF}$ [87], where $\Delta_{\rm CF}$ is the crystal-field splitting. Both are expected to be enlarged as J_H increases, which is in good agreement with the CDFT + U result.

The calculated Δ provides further understanding of magnetic transitions. Charge excitations in between $t_{2g\downarrow}$ and $t_{2g\uparrow}$ lead to the AFM interaction [2,3,42,75,88,89], and the enlarged $\Delta_{t_{2g\downarrow}-t_{2g\uparrow}}$ reduces the AFM coupling strength through $J \sim t^2/\Delta$. Similarly, the reduced $\Delta_{e_{g\uparrow}-e_{g\uparrow}}$ enhances the FM interaction. Traditionally these two are believed to be the main magnetic interactions in $LaMnO_3$, and therefore our results in Fig. 2(c) are consistent with the AFM-to-FM transition in Fig. 1(b) as a function of J_H. The transition from G-AFM to A-AFM order is related to the cooperative Jahn-Teller distortion and the orbital order. Due to the d_{x^2}/d_{y^2}-like orbital order in the xy plane, the e_g-e_g hopping, responsible for FM order, is stronger within the xy plane than along the z direction.

Another interesting feature found by comparing two phase diagrams in Fig. 1 is the calculated magnetic moment at the Mn site. Although the size of moment changes is not significant, SDFT + U and CDFT + U exhibit an opposite trend. With a fixed U value of 4.0 eV, for example, the Mn moment is reduced from $3.77\mu_B$ to $3.68\mu_B$ as J_H increases from 0.3 to 0.9 eV in SDFT + U. In CDFT + U, on the other hand, it is gradually increased from $3.30\mu_B$ to $3.69\mu_B$. This behavior is consistent with the opposite trend of $\Delta_{\downarrow\uparrow}$ shown in Figs. 2(b) and 2(c).

B. Electronic structure and lattice optimization

The calculated electronic structure by CDFT + U is presented in Fig. 3. We emphasize once again that this is a CDFT+U band-structure report for $LaMnO_3$ while all previous calculations were performed within the SDFT + U formalism [38–40,43,45,46,48–50,53–59,61,90–92]. The magnetic moment $\mu_{\rm Mn} = 3.62\mu_B$ and the gap $\Delta_{\rm gap} = 1.1$ eV are in good agreement with experimental values; $\mu_{\rm Mn}^{\rm exp} = 3.7 \pm 0.1\mu_B$ [70], $\Delta_{\rm gap}^{\rm exp} = 1.1$ eV [93], and 1.7 eV [94]. $\Delta_{e_{g\uparrow}-e_{g\uparrow}}$, $\Delta_{t_{2g\downarrow}-t_{2g\uparrow}}$, $\Delta_{e_{g\downarrow}-t_{2g\uparrow}}$, and $\Delta_{t_{2g\downarrow}-e_{g\uparrow}}$ are found to be 3.02, 4.62, 5.57, and 3.28 eV, respectively. The C-type d_{x^2}/d_{y^2} orbital order with $(\pi, \pi, 0)$ ordering vector is also well reproduced. The lowest excitation is of d-d character, which supports the recent

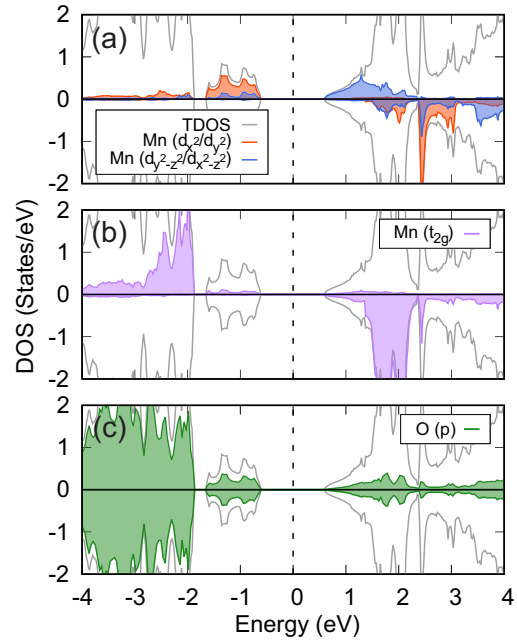

FIG. 3. (a)–(c) The calculated DOS by CDFT + U corresponding to the A-AFM ground-state spin order. cRPA values of $U = 4.0$ and $J_H = 0.7$ eV were used. The gray, red, blue, violet, and green colors represent the total DOS (divided by 4 for presentation), Mn-d_{x^2/y^2}, Mn-$d_{x^2-z^2/y^2-z^2}$, Mn-t_{2g}, and O-2p states, respectively. The zero energy corresponds to the Fermi level (vertical dashed line).

theoretical and experimental studies [17,19,20]. The oxygen states are mainly located in between −6.7 and −1.3 eV below the highest occupied state. If we use the significantly large $U \sim 8.0$–10.1 eV obtained from constrained LDA (cLDA) [38,40], the gap becomes a charge-transfer type as reported in a previous SDFT + U study [38].

It is useful to make a comparison to the result of SDFT+U. With cRPA parameters, SDFT + U gives $\mu_{\rm Mn}^{\rm SDFT+U} = 3.70\mu_B$ and $\Delta_{\rm gap}^{\rm SDFT+U} = 1.5$ eV. The Mott-Hubbard nature of the gap as well as the C-type d_{x^2}/d_{y^2} orbital order (not shown) are also consistent with the CDFT+U result. The significant differences are noticed in the detailed electronic structure. For example, the calculated $\Delta_{t_{2g\downarrow}-t_{2g\uparrow}} = 5.85$ eV is markedly larger than that of CDFT + U. It affects the spin-dependent energy level splittings and the magnetic interactions.

Even if CDFT + U provides a quite reasonable description of the electronic property, it is still challenging to describe $LaMnO_3$ within the fully first-principles framework. Note that in the above the experimental lattice structure has been used. We found that the lattice optimized within CDFT + U along with cRPA parameters overestimates the lattice constants and the volume by about 1–5 % in comparison to experiments. The Mn-O-Mn bond angle and the orthorhombicity [57] are underestimated and overestimated, respectively. A similar number of differences is also found in the SDFT + U result with cRPA parameters. This point has been double-checked with the plane-wave basis method using the VASP (Vienna *ab-initio* simulation package). The previous studies have been struggling with this same issue [40,43,45,54,59]. Due to the strong spin-charge-orbital and lattice couplings in

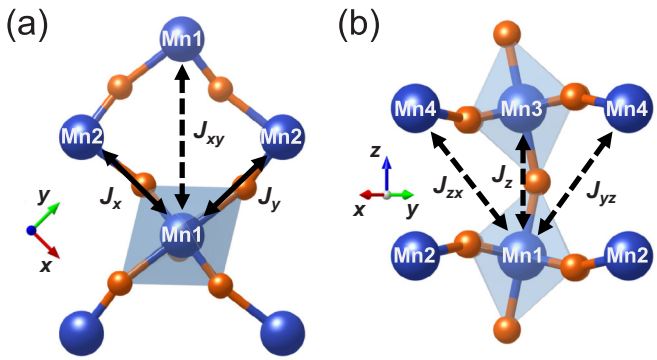

FIG. 4. (a), (b) The magnetic exchange couplings in $LaMnO_3$. The in-plane and out-of-plane first-neighbor interactions are denoted by $J_{x,y}$ and J_z, respectively. The second-neighbor couplings are denoted by J_{xy} (in-plane), J_{yz} (in-plane), and J_{zx} (out-of-plane).

this material, the fully self-consistent calculation for both the structural and electronic property becomes quite challenging. The difficulty can also be attributed to the cRPA process, which is separated from the other part of the self-consistent calculation and conducted at a given lattice geometry.

C. Magnetic interactions

1. The role of second-neighbor interactions

Magnetic interactions in $LaMnO_3$ have long been an issue of debate particularly for the second-neighbor interaction strength. In Refs. [47,52,55,57–59,89] it is argued that only the nearest-neighbor interactions [i.e., J_x, J_y, and J_z in Fig. 4(a)] are important to stabilize the A-AFM order. The second-neighbor J_{zx} and J_{yz} [see Fig. 4(a)] were either neglected or found to be small. In Refs. [40,42,61], on the other hand, these second-neighbor interactions were claimed to play the key role in stabilizing the ground-state spin order. Here we note that many different computational approaches and their combinations have been considered previously. The MFT calculation, based on LSDA (local spin-density approximation; $U = 0$) spin density, and the total energy calculations, based on the hybrid functional, support the significance of second-neighbor interactions [40,42,61]. On the contrary, the total energy calculations based on the *ab initio* Hartree-Fock approximation reports the negligible contribution from J_{zx} and J_{yz} [47]. It is noted that each of these techniques can give a different answer for the electronic structure. For example, *ab initio* Hartree-Fock produces the charge transfer type band gap while LSDA does the Mott-Hubbard type [40,42]. LSDA + U with cLDA interaction parameters does not reproduce the A-AFM ground state. With the hybrid functional, a reasonable size of the Mott-Hubbard gap is reproduced [61]. In this case, however, they reported that a different conclusion can be reached depending on the choices of metastable spin orders [61].

Here we performed MFT calculation based on our CDFT + U electronic structure with cRPA parameters. Note that CDFT+U electronic structure can give different results from SDFT+U [95]. Our result clearly shows that the second-neighbor interactions, J_{zx} and J_{yz}, are not essential for stabilizing the A-AFM spin order. The in-plane first-neighbor interaction is FM, $J_x = J_y = 1.34$ meV, while the out-of-plane is AFM, $J_z = -0.95$ meV [96]. The calculated $J_{xz} = J_{yz} = -0.27$ meV is AFM corresponding to 20% and 29% of J_x and J_z, respectively. It is important to note that even without these interactions ($J_{zx} = J_{yz} = 0$) the same ground-state spin order is stabilized. The in-plane second-neighbor interaction is small enough; $J_{xy} = -0.04$ (along the short-distance a-axis direction) and -0.17 meV (along the long-distance b-axis direction).

2. The orbital-decomposed results

The magnetic orders and their phase transitions in manganites have been studied from the point of view of the competition between FM e_g-e_g and AFM t_{2g}-t_{2g} interactions [2,3,42,74,75,97–99]. For instance, in undoped $LaMnO_3$, a strong FM e_g-e_g coupling wins over the in-plane (xy plane) AFM t_{2g}-t_{2g} coupling while it is weaker along the z direction largely due to the orbital order. This interaction profile provides a reasonable picture for the A-AFM spin ground state. From our calculation of orbital-decomposed magnetic couplings [85], the $J_{e_g\text{-}e_g}$ is indeed found to be FM; $J_{e_g\text{-}e_g} = 4.66$ and 2.32 meV within the xy plane and the out-of-plane, respectively (see Table I). $J_{t_{2g}\text{-}t_{2g}}$ is AFM; -1.56 and -3.03 meV for the in- and out-of-plane, respectively. Our result is therefore consistent with the prevailing current understanding.

It is remarkable to see the significant AFM $J_{e_g\text{-}t_{2g}}$ couplings in the sense that this interorbital interaction has largely been ignored in the previous studies [2,3,12,14,17,19,75,76,88,97,98,100–102]. Our calculation shows that the in-plane e_g-t_{2g} interaction $J_{x,y}(e_g\text{-}t_{2g}) = -1.76$ meV is larger than $J_{x,y}(t_{2g}\text{-}t_{2g}) = -1.56$ meV and $J_z(e_g\text{-}t_{2g}) = -0.24$ meV. While the possibility of non-negligible e_g-t_{2g} charge excitation was speculated in some of the literature [19,40,89], our calculation provides strong and quantitative evidence for that.

The $J_{e_g\text{-}t_{2g}}$ interaction is not directionally symmetric. For example, while J_x of Mn1(t_{2g})-Mn2(e_g) is -1.77 meV, J_x of Mn1(e_g)-Mn2(t_{2g}) is negligibly small (see Table I). Due to the significant $GdFeO_3$-type distortion and orbital order, the hopping integrals between e_g and t_{2g} orbitals can be nonzero and the two Mn sites are no longer equivalent. This is clearly different from the case of $CaMnO_3$. As a t_{2g}^3 system, the $CaMnO_3$ has no orbital order while it shares the $GdFeO_3$-type distortion with $LaMnO_3$. As a result, the e_g-t_{2g} interaction is negligible [103]. Our calculation shows that the neglect of e_g-t_{2g} coupling in $LaMnO_3$ can be an oversimplification [88,99].

TABLE I. The calculation results of orbital-decomposed nearest-neighbor J. For the definition of J_x, J_y, and J_z, see Fig. 3. The unit is meV.

		Mn2: J_x		Mn2: J_y		Mn3: J_z	
		e_g	t_{2g}	e_g	t_{2g}	e_g	t_{2g}
Mn1	e_g	4.66	0.01	4.66	−1.77	2.32	−0.12
	t_{2g}	−1.77	−1.56	0.01	−1.56	−0.12	−3.03

Our finding of e_g-t_{2g} AFM coupling has significant implications for understanding the rich phase diagram and their transitions. It is also important for the study of manganite surfaces, interfaces, and thin films where the different coordination and crystal field can significantly change the magnetic interaction profiles [31–34]. In the sense that the interorbital couplings can even be manipulated by strain, for example [9–12,14,57], it can have an implication for applications.

IV. SUMMARY

We revisit a classical CMR material, $LaMnO_3$, within the DFT + U method. While all the previous calculations were based on SDFT + U, the current study clearly shows that the use of charge-only density is crucial to properly describe the electronic structure and magnetic property. It is found that the nearest-neighbor interactions are enough to stabilize the A-AFM spin ground state contrary to a part of the previous studies. The orbital-resolved J_{ij} calculation shows that the e_g-t_{2g} interaction is quite significant.

ACKNOWLEDGMENTS

This work was supported by Basic Science Research Program through the National Research Foundation of Korea (NRF) funded by the Ministry of Education (Grant No. 2018R1A2B2005204).

[1] M. B. Salamon and M. Jaime, Rev. Mod. Phys. **73**, 583 (2001).
[2] E. Dagotto, *Nanoscale Phase Separation and Colossal Magnetoresistance* (Springer-Verlag, Berlin, 2003).
[3] T. Chatterji, *Colossal Magnetoresistive Manganites* (Springer, The Netherlands, 2004).
[4] E. Dagotto, New J. Phys. **7**, 67 (2005).
[5] Y. Tokura, Rep. Prog. Phys. **69**, 797 (2006).
[6] D. I. Khomskii, *Transition Metal Compounds* (Cambridge University Press, Cambridge, 2014).
[7] R. von Helmolt, J. Wecker, B. Holzapfel, L. Schultz, and K. Samwer, Phys. Rev. Lett. **71**, 2331 (1993).
[8] S. Jin, T. H. Tiefel, M. McCormack, R. A. Fastnacht, R. Ramesh, and L. H. Chen, Science **264**, 413 (1994).
[9] I. Loa, P. Adler, A. Grzechnik, K. Syassen, U. Schwarz, M. Hanfland, G. K. Rozenberg, P. Gorodetsky, and M. P. Pasternak, Phys. Rev. Lett. **87**, 125501 (2001).
[10] J. D. Fuhr, M. Avignon, and B. Alascio, Phys. Rev. Lett. **100**, 216402 (2008).
[11] M. Baldini, V. V. Struzhkin, A. F. Goncharov, P. Postorino, and W. L. Mao, Phys. Rev. Lett. **106**, 066402 (2011).
[12] M. Sherafati, M. Baldini, L. Malavasi, and S. Satpathy, Phys. Rev. B **93**, 024107 (2016).
[13] E. Saitoh, S. Okamoto, K. T. Takahashi, K. Tobe, K. Yamamoto, T. Kimura, S. Ishihara, S. Maekawa, and Y. Tokura, Nature (London) **410**, 180 (2001).
[14] K. H. Ahn and A. J. Millis, Phys. Rev. B **61**, 13545 (2000).
[15] K. Tobe, T. Kimura, Y. Okimoto, and Y. Tokura, Phys. Rev. B **64**, 184421 (2001).
[16] M. A. Quijada, J. R. Simpson, L. Vasiliu-Doloc, J. W. Lynn, H. D. Drew, Y. M. Mukovskii, and S. G. Karabashev, Phys. Rev. B **64**, 224426 (2001).
[17] N. N. Kovaleva, A. V. Boris, C. Bernhard, A. Kulakov, A. Pimenov, A. M. Balbashov, G. Khaliullin, and B. Keimer, Phys. Rev. Lett. **93**, 147204 (2004).
[18] M. W. Kim, P. Murugavel, S. Parashar, J. S. Lee, and T. W. Noh, New J. Phys. **6**, 156 (2004).
[19] N. N. Kovaleva, A. M. Oleś, A. M. Balbashov, A. Maljuk, D. N. Argyriou, G. Khaliullin, and B. Keimer, Phys. Rev. B **81**, 235130 (2010).
[20] A. S. Moskvin, A. A. Makhnev, L. V. Nomerovannaya, N. N. Loshkareva, and A. M. Balbashov, Phys. Rev. B **82**, 035106 (2010).
[21] B. R. K. Nanda and S. Satpathy, Phys. Rev. B **81**, 174423 (2010).
[22] E. Pavarini and E. Koch, Phys. Rev. Lett. **104**, 086402 (2010).
[23] A. Flesch, G. Zhang, E. Koch, and E. Pavarini, Phys. Rev. B **85**, 035124 (2012).
[24] S. Smadici, P. Abbamonte, A. Bhattacharya, X. Zhai, B. Jiang, A. Rusydi, J. N. Eckstein, S. D. Bader, and J.-M. Zuo, Phys. Rev. Lett. **99**, 196404 (2007).
[25] X. Zhai, C. S. Mohapatra, A. B. Shah, J.-M. Zuo, and J. N. Eckstein, Adv. Mater. **22**, 1136 (2010).
[26] J. Garcia-Barriocanal, F. Y. Bruno, A. Rivera-Calzada, Z. Sefrioui, N. M. Nemes, M. Garcia-Hernández, J. Rubio-Zuazo, G. R. Castro, M. Varela, S. J. Pennycook, C. Leon, and J. Santamaria, Adv. Mater. **22**, 627 (2010).
[27] J. Garcia-Barriocanal, J. C. Cezar, F. Y. Bruno, P. Thakur, N. B. Brookes, C. Utfeld, A. Rivera-Calzada, S. R. Giblin, J. W. Taylor, J. A. Duffy, S. B. Dugdale, T. Nakamura, K. Kodama, C. Leon, S. Okamoto, and J. Santamaria, Nat. Commun. **1**, 82 (2010).
[28] M. Gibert, P. Zubko, R. Scherwitzl, J. Íñiguez, and J.-M. Triscone, Nat. Mater. **11**, 195 (2012).
[29] A. T. Lee and M. J. Han, Phys. Rev. B **88**, 035126 (2013).
[30] P. Di Pietro, J. Hoffman, A. Bhattacharya, S. Lupi, and A. Perucchi, Phys. Rev. Lett. **114**, 156801 (2015).
[31] X. R. Wang, C. J. Li, W. M. Lü, T. R. Paudel, D. P. Leusink, M. Hoek, N. Poccia, A. Vailionis, T. Venkatesan, J. M. D. Coey, E. Y. Tsymbal, Ariando, and H. Hilgenkamp, Science **349**, 716 (2015).
[32] J. J. Peng, C. Song, F. Li, Y. D. Gu, G. Y. Wang, and F. Pan, Phys. Rev. B **94**, 214404 (2016).
[33] Y. Anahory, L. Embon, C. J. Li, S. Banerjee, A. Meltzer, H. R. Naren, A. Yakovenko, J. Cuppens, Y. Myasoedov, M. L. Rappaport, M. E. Huber, K. Michaeli, T. Venkatesan, Ariando, and E. Zeldov, Nat. Commun. **7**, 12566 (2016).
[34] Z. Chen, Z. Chen, Z. Q. Liu, M. E. Holtz, C. J. Li, X. R. Wang, W. M. Lü, M. Motapothula, L. S. Fan, J. A. Turcaud, L. R. Dedon, C. Frederick, R. J. Xu, R. Gao, A. A. N'Diaye, E. Arenholz, J. A. Mundy, T. Venkatesan, D. A. Muller, L.-W. Wang, J. Liu, and L. W. Martin, Phys. Rev. Lett. **119**, 156801 (2017).
[35] J. Chakhalian, J. W. Freeland, A. J. Millis, C. Panagopoulos, and J. M. Rondinelli, Rev. Mod. Phys. **86**, 1189 (2014).

[36] A. Bhattacharya and S. J. May, Annu. Rev. Mater. Res. **44**, 65 (2014).

[37] D. D. Sarma, N. Shanthi, S. R. Barman, N. Hamada, H. Sawada, and K. Terakura, Phys. Rev. Lett. **75**, 1126 (1995).

[38] S. Satpathy, Z. S. Popović, and F. R. Vukajlović, Phys. Rev. Lett. **76**, 960 (1996).

[39] S. Satpathy, Z. S. Popović, and F. R. Vukajlović, J. Appl. Phys. **79**, 4555 (1996).

[40] I. Solovyev, N. Hamada, and K. Terakura, Phys. Rev. B **53**, 7158 (1996).

[41] W. E. Pickett and D. J. Singh, Phys. Rev. B **53**, 1146 (1996).

[42] I. Solovyev, N. Hamada, and K. Terakura, Phys. Rev. Lett. **76**, 4825 (1996).

[43] H. Sawada, Y. Morikawa, K. Terakura, and N. Hamada, Phys. Rev. B **56**, 12154 (1997).

[44] D. J. Singh and W. E. Pickett, Phys. Rev. B **57**, 88 (1998).

[45] H. Sawada and K. Terakura, Phys. Rev. B **58**, 6831 (1998).

[46] W. Y. Hu, M. C. Qian, Q. Q. Zheng, H. Q. Lin, and H. K. Wong, Phys. Rev. B **61**, 1223 (2000).

[47] Y.-S. Su, T. A. Kaplan, S. D. Mahanti, and J. F. Harrison, Phys. Rev. B **61**, 1324 (2000).

[48] I. S. Elfimov, V. I. Anisimov, and G. A. Sawatzky, Phys. Rev. Lett. **82**, 4264 (1999).

[49] P. Benedetti, J. van den Brink, E. Pavarini, A. Vigliante, and P. Wochner, Phys. Rev. B **63**, 060408 (2001).

[50] P. Ravindran, A. Kjekshus, H. Fjellvåg, A. Delin, and O. Eriksson, Phys. Rev. B **65**, 064445 (2002).

[51] H. Zenia, G. A. Gehring, and W. M. Temmerman, New J. Phys. **7**, 257 (2005).

[52] R. A. Evarestov, E. A. Kotomin, Y. A. Mastrikov, D. Gryaznov, E. Heifets, and J. Maier, Phys. Rev. B **72**, 214411 (2005).

[53] W.-G. Yin, D. Volja, and W. Ku, Phys. Rev. Lett. **96**, 116405 (2006).

[54] T. Hashimoto, S. Ishibashi, and K. Terakura, Phys. Rev. B **82**, 045124 (2010).

[55] C. Franchini, R. Kováčik, M. Marsman, S. S. Murthy, J. He, C. Ederer, and G. Kresse, J. Phys.: Condens. Matter **24**, 235602 (2012).

[56] L. Uba, S. Uba, L. P. Germash, L. V. Bekenov, and V. N. Antonov, Phys. Rev. B **85**, 125124 (2012).

[57] J. H. Lee, K. T. Delaney, E. Bousquet, N. A. Spaldin, and K. M. Rabe, Phys. Rev. B **88**, 174426 (2013).

[58] Y. S. Hou, H. J. Xiang, and X. G. Gong, Phys. Rev. B **89**, 064415 (2014).

[59] T. A. Mellan, F. Corà, R. Grau-Crespo, and S. Ismail-Beigi, Phys. Rev. B **92**, 085151 (2015).

[60] M. An, Y. Weng, H. Zhang, J.-J. Zhang, Y. Zhang, and S. Dong, Phys. Rev. B **96**, 235112 (2017).

[61] R. Kováčik, S. S. Murthy, C. E. Quiroga, C. Ederer, and C. Franchini, Phys. Rev. B **93**, 075139 (2016).

[62] J. Chen, A. J. Millis, and C. A. Marianetti, Phys. Rev. B **91**, 241111 (2015).

[63] H. Park, A. J. Millis, and C. A. Marianetti, Phys. Rev. B **92**, 035146 (2015).

[64] H. Chen and A. J. Millis, Phys. Rev. B **93**, 045133 (2016).

[65] S. Ryee and M. J. Han, Sci. Rep. **8**, 9559 (2018).

[66] V. I. Anisimov, J. Zaanen, and O. K. Andersen, Phys. Rev. B **44**, 943 (1991).

[67] A. I. Liechtenstein, V. I. Anisimov, and J. Zaanen, Phys. Rev. B **52**, R5467(R) (1995).

[68] J. P. Perdew, K. Burke, and M. Ernzerhof, Phys. Rev. Lett. **77**, 3865 (1996).

[69] V. I. Anisimov, I. V. Solovyev, M. A. Korotin, M. T. Czyżyk, and G. A. Sawatzky, Phys. Rev. B **48**, 16929 (1993).

[70] J. B. A. A. Elemans, B. Van Laar, K. R. Van Der Veen, and B. O. Loopstra, J. Solid State Chem. **3**, 238 (1971).

[71] http://www.openmx-square.org/.

[72] D. Vanderbilt, Phys. Rev. B **41**, 7892 (1990).

[73] S. G. Louie, S. Froyen, and M. L. Cohen, Phys. Rev. B **26**, 1738 (1982).

[74] L. F. Feiner and A. M. Oleś, Phys. Rev. B **59**, 3295 (1999).

[75] A. M. Oleś, G. Khaliullin, P. Horsch, and L. F. Feiner, Phys. Rev. B **72**, 214431 (2005).

[76] G. Khaliullin, Prog. Theor. Phys. **160**, 155 (2005).

[77] F. Aryasetiawan, M. Imada, A. Georges, G. Kotliar, S. Biermann, and A. I. Lichtenstein, Phys. Rev. B **70**, 195104 (2004).

[78] E. Şaşioğlu, C. Friedrich, and S. Blügel, Phys. Rev. B **83**, 121101(R) (2011).

[79] https://github.com/tkotani/ecalj.

[80] L. Vaugier, H. Jiang, and S. Biermann, Phys. Rev. B **86**, 165105 (2012).

[81] R. Sakuma and F. Aryasetiawan, Phys. Rev. B **87**, 165118 (2013).

[82] B. Amadon, T. Applencourt, and F. Bruneval, Phys. Rev. B **89**, 125110 (2014).

[83] A. I. Liechtenstein, M. I. Katsnelson, V. P. Antropov, and V. A. Gubanov, J. Magn. Magn. Mater. **67**, 65 (1987).

[84] M. J. Han, T. Ozaki, and J. Yu, Phys. Rev. B **70**, 184421 (2004).

[85] H. Yoon, T. J. Kim, J.-H. Sim, S. W. Jang, T. Ozaki, and M. J. Han, Phys. Rev. B **97**, 125132 (2018).

[86] For simplicity, we represented all the interorbital exchange interactions by a single parameter J_H. Then the $e_{g\downarrow}$-$t_{2g\uparrow}$ excitation, $(t^3_{2g\uparrow}e^1_{g\uparrow})(t^3_{2g\downarrow}e^1_{g\downarrow}) \rightleftarrows (t^2_{2g\uparrow}e^1_{g\uparrow})(t^3_{2g\downarrow}e^1_{g\downarrow}e^1_{g\uparrow})$, can be expressed by the interaction energies of $t^3_{2g\uparrow}e^1_{g\uparrow}$, $t^2_{2g\uparrow}e^1_{g\uparrow}$, and $t^3_{2g\downarrow}e^1_{g\downarrow}e^1_{g\uparrow}$, which are given by $6U' - 6J_H$, $3U' - 3J_H$, and $U + 9U' - 6J_H$, respectively. Thus the excitation energy is $U + 3J_H + \Delta_{\mathrm{CF}}$. Here U' is on-site interorbital direct Coulomb interaction.

[87] Similarly, the excitation energy of $(t^3_{2g\uparrow}e^1_{g\uparrow})(t^3_{2g\downarrow}e^1_{g\downarrow}) \rightleftarrows (t^3_{2g\uparrow}e^0_{g\uparrow})(t^3_{2g\downarrow}t^1_{2g\uparrow}e^1_{g\downarrow})$ is given by $6U' - 6J_H$, $3U' - 3J_H$, and $U + 9U' - 6J_H$.

[88] S. Ishihara, J. Inoue, and S. Maekawa, Phys. Rev. B **55**, 8280 (1997).

[89] I. Solovyev, J. Phys. Soc. Jpn. **78**, 054710 (2009).

[90] J. E. Medvedeva, M. A. Korotin, V. I. Anisimov, and A. J. Freeman, Phys. Rev. B **65**, 172413 (2002).

[91] G. Trimarchi and N. Binggeli, Phys. Rev. B **71**, 035101 (2005).

[92] C. Ederer, C. Lin, and A. J. Millis, Phys. Rev. B **76**, 155105 (2007).

[93] T. Arima, Y. Tokura, and J. B. Torrance, Phys. Rev. B **48**, 17006 (1993).

[94] T. Saitoh, A. E. Bocquet, T. Mizokawa, H. Namatame, A. Fujimori, M. Abbate, Y. Takeda, and M. Takano, Phys. Rev. B **51**, 13942 (1995).

[95] S. Keshavarz, J. Schött, A. J. Millis, and Y. O. Kvashnin, Phys. Rev. B **97**, 184404 (2018).
[96] SDFT + U calculations with cRPA parameters give the in-plane nearest-neighbor interaction $J_x = J_y = 1.62$ meV and the out-of-plane $J_z = -0.20$ meV.
[97] S. Yunoki, T. Hotta, and E. Dagotto, Phys. Rev. Lett. **84**, 3714 (2000).
[98] T. Hotta, M. Moraghebi, A. Feiguin, A. Moreo, S. Yunoki, and E. Dagotto, Phys. Rev. Lett. **90**, 247203 (2003).
[99] C. Lin and A. J. Millis, Phys. Rev. B **78**, 174419 (2008).
[100] A. J. Millis, Phys. Rev. B **53**, 8434 (1996).
[101] Z. Popovic and S. Satpathy, Phys. Rev. Lett. **84**, 1603 (2000).
[102] M. Snamina and A. M. Oleś, Phys. Rev. B **97**, 104417 (2018).
[103] S. Keshavarz, Y. O. Kvashnin, D. C. M. Rodrigues, M. Pereiro, I. Di Marco, C. Autieri, L. Nordström, I. V. Solovyev, B. Sanyal, and O. Eriksson, Phys. Rev. B **95**, 115120 (2017).